



Research article

Creation of hidden n -scroll Lorenz-like attractors

Jun Pan^{1,*}, Haijun Wang^{2,*} and Feiyu Hu³

¹ School of Science, Zhejiang University of Science and Technology, Hangzhou 310023, China

² School of Electronic and Information Engineering (School of Big Data Science), Taizhou University, Taizhou 318000, China

³ College of Sustainability and Tourism, Ritsumeikan Asia Pacific University, Beppu 874-8577, Japan

* **Correspondence:** Email: panjun@zust.edu.cn, 2021033@tzc.edu.cn.

Abstract: Compared with the recently reported hidden two-scroll Lorenz-like attractors in symmetric quadratic and sub-quadratic Lorenz-like dynamical systems, little seems to be concerned with the generation of hidden n -scroll ($n \in \mathbb{N}$) attractors as far as one knows, especially the one whose number of scrolls equals the one of equilibria. To achieve this target, we first constructed a new asymmetric quadratic Lorenz-like analogue and seized hidden single-scroll Lorenz-like attractors, which were also created through the collapse of pseudo singularly degenerate heteroclinic cycles. Then, utilizing the fractal process or rotation symmetry, the proposed system may exhibit hidden n -scroll Lorenz-like attractors coexisting with n stable equilibria, and two examples of hidden two/three-scroll Lorenz-like attractors coexisting with two/three stable equilibria were given. In addition, the existence of a single heteroclinic orbit was proved with the help of suitable Lyapunov functions. The obtained results may not only generalize the second part of Hilbert's 16th problem (i.e., the degree may determine the geometrical structure of strange attractors), but also provide reference for practical application.

Keywords: extension of the second part of Hilbert's 16th problem; hidden n -scroll Lorenz-like attractor; asymmetric pseudo singularly degenerate heteroclinic cycle; heteroclinic orbit; Lyapunov function

1. Introduction

Dated back to 1993, Miranda and Stone introduced the method of fractal process or rotation symmetry and constructed a quotient of the Lorenz dynamical system or proto-Lorenz system, leading to the emergence of self-excited n -scroll Lorenz attractors [1]. In the same way, other researchers obtained self-excited twofold and threefold cover of the Rössler attractors [2], self-excited $4n$ -wing Qi attractors [3], and $2n$ -wing Lorenz-like attractors with $2n$ stable equilibria or no equilibrium point [4], and $2n$ -wing concealed Lorenz-based chemical attractors ($n \in \mathbb{N}$) [5]. Meanwhile, the self-excited n -scroll Lorenz-

like attractors can be generated through the recently reported single-scroll Lorenz-like attractors by Pan et al. [6].

Remarkably, few studies have been done on the creation of hidden n -scroll Lorenz-like attractors. Motivated by the generalization of the second part of Hilbert's celebrated 16th problem [7, 8] (i.e., the degree of polynomials in the studied models may determine the number and mutual disposition of attractors and repellers, if they exist), Wang et al. guessed that the decrease of powers of some certain variables may enlarge the range of some parameters of hidden attractors, and verified it via an example of a six-fifths-degree sub-quadratic Lorenz-like system [9]. As done in [1], one can transform a two-scroll hidden Lorenz-like attractor into a hidden proto-Lorenz-like attractor, and arrive at hidden n -scroll Lorenz-like attractors using rotation symmetry.

Jafari et al. reviewed three new rare chaotic flows with hidden attractors coexisting with (1) no equilibrium, (2) a line of equilibrium points, and (3) a stable equilibrium [10]. Dudkowski et al. also reported hidden attractors in different complex dynamical systems [11]. Chowdhury and Ghosh coined hidden attractors with no equilibria from a novel autonomous 3D periodically forced system [12]. Chowdhury et al. further found multi-stability in an ecological multi-games model [13]. Wang et al. demonstrated a large number of coexisting chaotic attractors in a discrete fractional Hopfield neural network (HNN) memristive neural network with three neurons [14]. Deng et al. discovered the coexistence of diverse attractors, such as heterogeneous, symmetric, and initial offset-boosted attractors from a memristor-coupled heterogeneous Tabu learning neuronal network (MCTLNN) comprising distinct types of Tabu learning neurons [15]. Moreover, they also generated the multi-wing butterfly chaotic attractor in the memristive HNN [16]. Therefore, it is worthwhile to coin multi-scroll Lorenz-like attractors from the viewpoint of both theory and application.

In this paper, we aim to construct a new three-dimensional quadratic Lorenz-like system yet with hidden single-scroll Lorenz-like attractors coexisting with the unstable origin and a stable nontrivial equilibrium point, and then apply rotation symmetry to create hidden n -scroll Lorenz-like attractors coexisting with n stable equilibria. On the one hand, few literatures discussed such types of Lorenz-like systems as far as we know, which may also provide reference for applications involving hidden Lorenz-like attractors on the other hand, i.e., data-driven predictions of the Lorenz-like systems [17, 18]. For these reasons, the study of hidden single-scroll Lorenz-like attractors is of theoretical and practical value, motivating the content of the present work.

In order to increase the chances of finding the targeted model, it should satisfy the following three principles:

(1) The system should be similar to the Lorenz-like analogues [9] but be asymmetric, which may ensure the single-scroll attractors.

(2) The degree of some variable states should be $2n$ to the $(2n+1)$ th power, which might guarantee the existence of hidden attractors.

(3) The system should retain some key dynamics, i.e., pseudo or true singularly degenerate heteroclinic cycles, which may be the route to the hidden single-scroll Lorenz-like attractors.

In light of the three simple tips and a trial-and-error process, we have coined the hidden single-scroll Lorenz-like attractor in a new 3D quadratic Lorenz-like system yet with the term $c\sqrt[7]{x^6}$, which falls in the second and third categories [19]. Our main contributions are listed as follows:

(1) Finding a kind of quadratic Lorenz-like system with hidden single-scroll attractors coexisting with a single stable equilibrium point and the unstable origin, i.e., the protos of the ones creating hidden

n -scroll attractors coexisting with n stable equilibria under the rotation symmetry.

(2) Explaining the formation of hidden single-scroll Lorenz-like attractors to some degree, i.e., collapses of pseudo singularly degenerate heteroclinic cycles.

(3) Proving the existence of a single heteroclinic orbit to the unstable origin and a stable nontrivial equilibrium point.

(4) Enriching the second part of Hilbert's celebrated 16th problem, i.e., the degree determining the geometrical structure of the attractor.

The content of this article includes the following: Some basic concepts are introduced in Section 1. Section 2 formulates the new simple asymmetric Lorenz-like system and introduces the main results, including hidden single-scroll Lorenz-like attractors coexisting with the unstable origin and a single stable nontrivial equilibria, n -scroll Lorenz-like attractors coexisting with n stable nontrivial equilibria ($n > 1$), and in particular hidden one/two/three-scroll Lorenz-like attractors. Section 3 illustrates asymmetric pseudo singularly degenerate heteroclinic cycles, explaining the formation of hidden single-scroll Lorenz-like attractors to some degree. Utilizing appropriate Lyapunov functions, the existence of a single heteroclinic orbit to the unstable origin and a stable nontrivial equilibrium point is proved when $b \geq 2a > 0$ and $c \neq 0$ in Section 4. Finally, we draw conclusions and inquire into future work in Section 5.

2. Preliminaries

In this paper, system (3.1) has a line of semi-hyperbolic equilibria $E_z = \{(0, 0, z) | z \in \mathbb{R}\}$ (i.e., the z -axis) which is unstable when $c \neq 0$. The true singularly degenerate heteroclinic cycle is defined to be an invariant set consisting of a line (resp. curve) of equilibria and a heteroclinic orbit connecting two equilibria in this line (resp. curve) [20, 21], while the pseudo one ultimately tends to infinity after a short-duration transient of singularly degenerate heteroclinic cycles [22].

As defined in [1–5], fractal process or rotation symmetry refer to the mapping $\Psi_n : (x, y, z) \rightarrow (Re(x + iy)^n, Im(x + iy)^n, z)$, $n \in \mathbb{N}$.

From a computational perspective and based on the simplicity of finding their basins of attraction in the phase space, an attractor of a system is typically divided into two different regimes: the self-excited and the hidden attractor. The former is where its basin of attraction intersects with any open neighborhood of a stationary state (an equilibrium), and otherwise, we have the latter [7].

As the ones in [6, 9, 22–27] and the references therein, the method adopted for proving the existence of heteroclinic orbits is a combination of the Lyapunov function and concepts of a ω -limit set and α -limit set. Namely, the unstable manifolds of E_0 tending to globally stable E' create a single orbit heteroclinic to E_0 and E' .

3. The new 3D asymmetric quadratic Lorenz-like system and our main results

Introducing the nonlinear term $c\sqrt[7]{x^6}$ to the Lorenz system family, the following simple 3D asymmetric analogue is formulated:

$$\begin{cases} \dot{x} = a(y - x), \\ \dot{y} = c\sqrt[7]{x^6} - xz, \\ \dot{z} = -bz + xy, \end{cases} \quad (3.1)$$

where $a \neq 0$ and $b, c \in \mathbb{R}$. In order to detect the hidden attractors and other complicated dynamics, we will first discuss the distribution of equilibrium points, local stability, and bifurcation of them in the following propositions:

Proposition 3.1. *The distribution of equilibrium points of system (3.1) is listed in Table 1, where $E_0 = (0, 0, 0)$, $E_z = \{(0, 0, z) | z \in \mathbb{R}\}$, and $E' = (\sqrt[15]{bc^7}, \sqrt[15]{bc^7}, \frac{\sqrt[15]{(bc)^{14}}}{b})$.*

Table 1. Distribution of equilibria of system (3.1).

b	c	Equilibria
$= 0$		E_z
$\neq 0$	$= 0$	E_0
	$\neq 0$	E_0, E'

Proposition 3.2. (1) When $a \neq 0$ and $(b, c) \in \mathbb{R}^2$, Table 2 gives the local dynamics of E_0 .

(2) When $c \neq 0$, all of E_z are unstable.

(3) When $bc \neq 0$, Table 3 presents the local behaviors of E' , where $W = \{(a, b, c) | abc \neq 0\}$, $W_1 = \{(a, b, c) \in W | a + b > 0, ab + (1 + \frac{a}{7b}) \sqrt[15]{(bc)^{14}} > 0, a \sqrt[15]{(bc)^{14}} > 0\}$, $W_2 = W \setminus W_1$, and

$$W_1^1 = \{(a, b, c) \in W_1 | ab(a + b) + (b - a + \frac{a^2}{7b}) \sqrt[15]{(bc)^{14}} > 0\},$$

$$W_1^2 = \{(a, b, c) \in W_1 | c = \pm \frac{1}{b} \sqrt[14]{(\frac{7ab^2(a+b)}{7b(a-b)-a^2})^{15}} \triangleq \pm c_*\},$$

$$W_1^3 = \{(a, b, c) \in W_1 | ab(a + b) + (b - a + \frac{a^2}{7b}) \sqrt[15]{(bc)^{14}} < 0\}.$$

Remark 1. (1) Proposition 3.2 directly follows from linear analysis, the Routh-Hurwitz criterion, and the project method [28, 29], i.e., the characteristic equation of E_0 : $(\lambda + b)(\lambda^2 + a\lambda - a(\frac{6c}{7\sqrt[15]{x}} - z)) = 0$ when $x, z \rightarrow 0$, the one of E_z : $\lambda(\lambda^2 + a\lambda - a(\frac{6c}{7\sqrt[15]{x}} - z)) = 0$ when $x \rightarrow 0, z \in \mathbb{R}$, and the one of E' : $\lambda^3 + (a + b)\lambda^2 + [ab + (1 + \frac{a}{9b}) \sqrt[19]{(bc)^{18}}]\lambda + \frac{19a \sqrt[19]{(bc)^{18}}}{9} = 0$. In particular, interested readers can resort to the project method to study the Hopf bifurcation of E' .

(2) Since each one of E_z is unstable, the true singularly degenerate heteroclinic cycles are nonexistent in system (3.1). However, the pseudo ones, i.e., a short-duration transient of singularly degenerate heteroclinic cycles approaching infinity, may exist as another Lorenz-like system [22].

Table 2. The local behaviors of E_0 .

b	a	c	Property of E_0
< 0	< 0	$= 0$	A 1D W_{loc}^c and a 2D W_{loc}^u
		$\neq 0$	A 1D W_{loc}^s and a 2D W_{loc}^u
	> 0	$= 0$	A 1D W_{loc}^s , a 1D W_{loc}^c , and a 1D W_{loc}^u
		$\neq 0$	A 1D W_{loc}^s and a 2D W_{loc}^u
> 0	< 0	$= 0$	A 1D W_{loc}^s , a 1D W_{loc}^c , and a 1D W_{loc}^u
		$\neq 0$	A 2D W_{loc}^s and a 1D W_{loc}^u
	> 0	$= 0$	A 2D W_{loc}^s and a 1D W_{loc}^c
		$\neq 0$	A 2D W_{loc}^s and a 1D W_{loc}^u

Table 3. Local dynamics of E' .

(a, c, b)	Property of E'
W_1^1	Asymptotically stable
W_1^2	Hopf bifurcation
$W_1^3 \cup W_2$	Unstable

Set $(a, b) = (4, 1)$. By Propositions 3.2–3.3, E_0 is unstable, and E' is stable (resp. unstable) when $0 < |c| < 35.5244$ (resp. $|c| > 35.5244$) and Hopf bifurcation occurs when $c = \pm 35.5244$. Choosing the initial points $(x_0^{1,2}, y_0^{1,2}, z_0^1) = (\pm 1.314, \pm 1.618, 1.618) \times 10^{-7}$, $(x_0^{3,4}, y_0^{3,4}, z_0^2) = (\pm 8.834, \pm 6.607, 28.12)$ and using MATLAB's procedure ode45 with the same relative and absolute tolerance 10^{-6} , Figures 1–4 may illustrate the existence of hidden single-scroll Lorenz-like attractors in system (3.1) when some $|c| \in [23.9, 24.8]$.

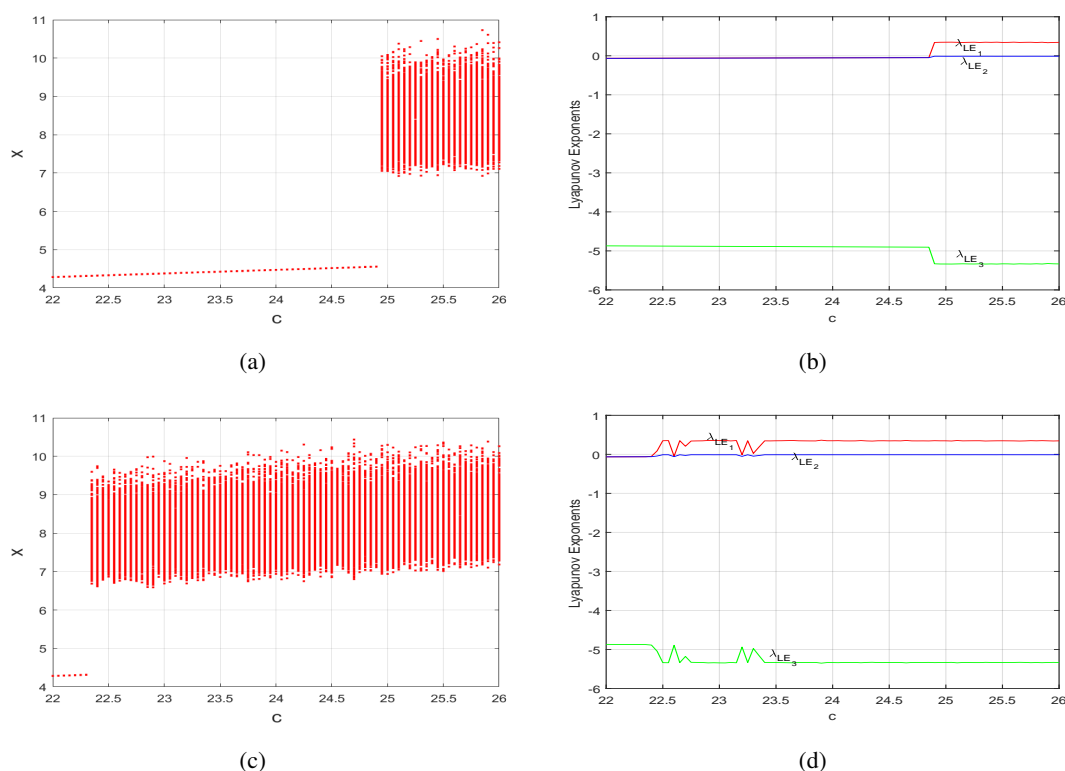


Figure 1. When $(a, b) = (4, 1)$ and $c \in [22, 26]$, (a), (b) $(x_0^1, y_0^1, z_0^1) = (1.314, 1.618, 1.618) \times 10^{-7}$, (c), (d) $(x_0^3, y_0^3, z_0^2) = (8.834, 6.607, 28.12)$, bifurcation diagrams and Lyapunov exponents versus c of system (3.1), illustrating hidden Lorenz-like attractors coexisting with unstable E_0 and stable E' in system (3.1).

Next, with the fractal process or rotation symmetry [1–5]: Ψ_n , $n = 2, 3, \dots$, system (3.1) may illustrate hidden n -scroll Lorenz-like attractors coexisting with n stable equilibria. Here, we only exhibit

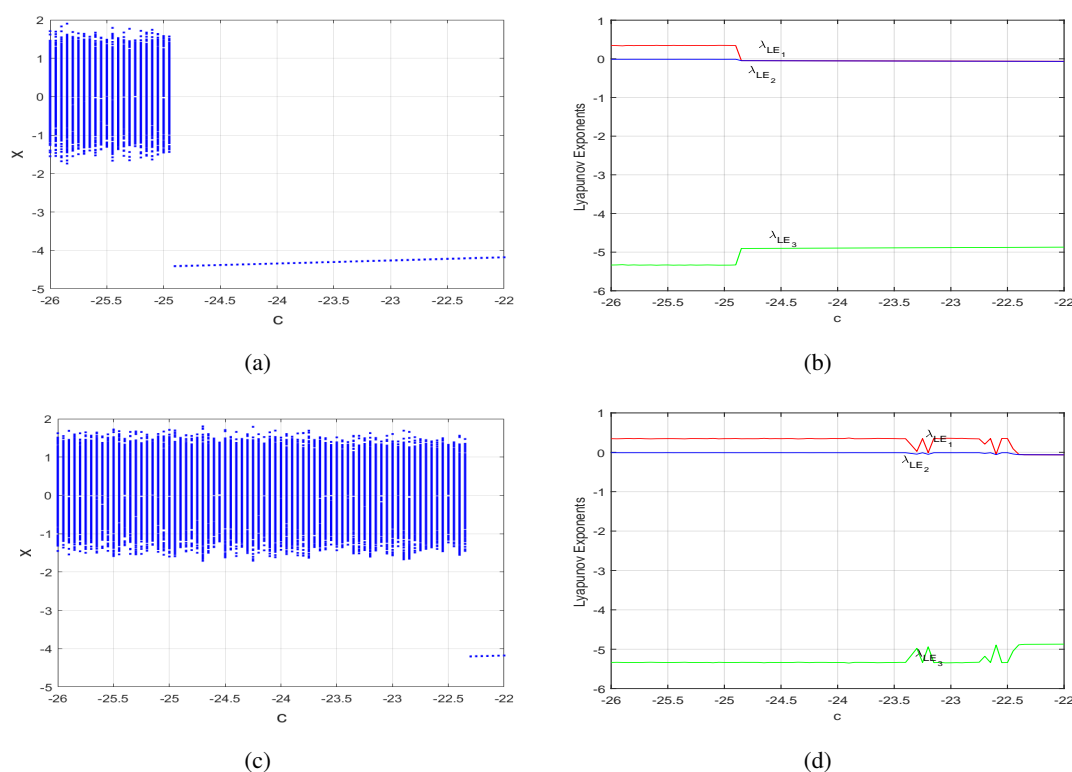


Figure 2. When $(a, b) = (4, 1)$ and $c \in [-26, -22]$, (a), (b) $(x_0^2, y_0^2, z_0^1) = (-1.314, -1.618, 1.618) \times 10^{-7}$, (c), (d) $(x_0^4, y_0^4, z_0^2) = (-8.834, -6.607, 28.12)$, bifurcation diagrams and Lyapunov exponents versus c of system (3.1), suggesting the existence of the hidden Lorenz-like attractors coexisting with unstable E_0 and stable E' in system (3.1).

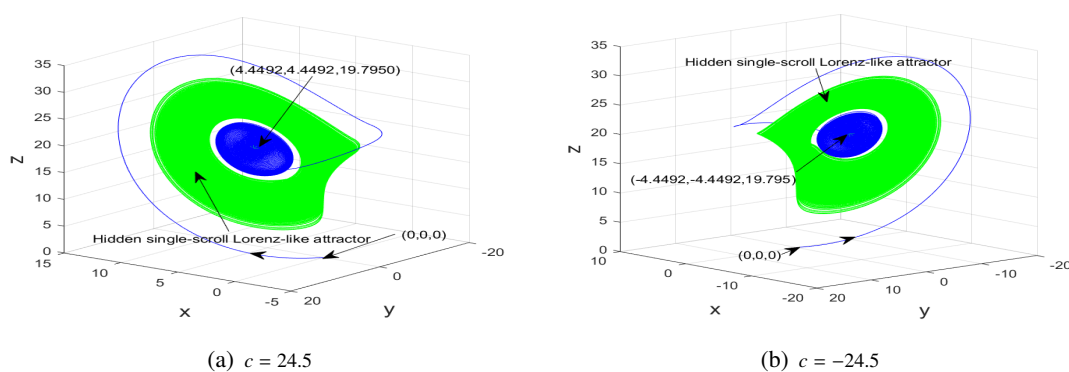


Figure 3. Phase portraits of system (3.1) with $(a, b) = (4, 1)$, (a) $c = 24.5$, $(x_0^1, y_0^1, z_0^1) = (1.314, 1.618, 1.618) \times 10^{-7}$ (colored in blue) and $(x_0^3, y_0^3, z_0^2) = (8.834, 6.607, 28.12)$ (colored in green), (b) $c = -24.5$, $(x_0^2, y_0^2, z_0^1) = (-1.314, -1.618, 1.618) \times 10^{-7}$ (colored in blue) and $(x_0^4, y_0^4, z_0^2) = (-8.834, -6.607, 28.12)$ (colored in green), illustrating the existence of hidden single-scroll Lorenz-like attractors coexisting with unstable E_0 and stable E' suggested in Figures 1 and 2.

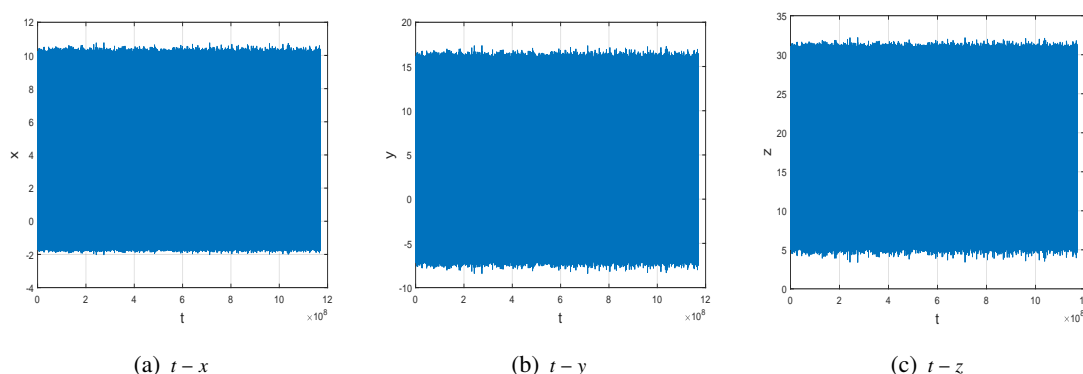


Figure 4. Time series of the hidden single-scroll Lorenz-like attractor coexisting with unstable E_0 and stable E' depicted in Figure 3(a) for integration time span $t = [0, 7 \times 10^6]$: (a) $t - x$, (b) $t - y$, (c) $t - z$, verifying that it is a sustained chaotic set rather than a transient chaotic set.

two examples of $n = 2, 3$, i.e., the following resulting systems of system (3.1):

$$\begin{cases} \dot{x} = \frac{1}{2(x^2+y^2)}[ax(2xy - x^2 + y^2) + y(c\sqrt[7]{(x^2 - y^2)^6} - (x^2 - y^2)z)], \\ \dot{y} = \frac{1}{2(x^2+y^2)}[-ay(2xy - x^2 + y^2) + x(c\sqrt[7]{(x^2 - y^2)^6} - (x^2 - y^2)z)], \\ \dot{z} = -bz + 2xy(x^2 - y^2), \end{cases} \quad (3.2)$$

and

$$\begin{cases} \dot{x} = \frac{1}{3(x^2+y^2)^2}[a(x^2 - y^2)(3x^2y - y^3 - x^3 + 3xy^2) + 2xy(c\sqrt[7]{(x^3 - 3xy^2)^6} - (x^3 - 3xy^2)z)], \\ \dot{y} = \frac{1}{3(x^2+y^2)^2}[-2axy(3x^2y - y^3 - x^3 + 3xy^2) + (x^2 - y^2)(c\sqrt[7]{(x^3 - 3xy^2)^6} - (x^3 - 3xy^2)z)], \\ \dot{z} = -bz + (x^3 - 3xy^2)(3x^2y - y^3). \end{cases} \quad (3.3)$$

Figures 5 and 6 illustrate hidden two/three-scroll Lorenz-like attractors coexisting with two/three stable equilibria of system (3.1) using system (3.2)–(3.3).

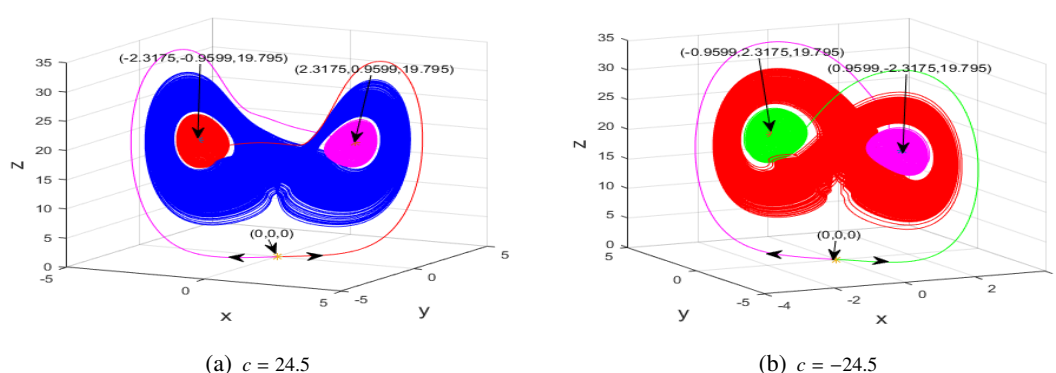


Figure 5. For $(a, b) = (4, 1)$, $(x_0^{5,6}, y_0^{5,6}, z_0^3) = (\pm 1.314, \pm 1.618, 1.618) \times 10^{-4}$, (a) $c = 24.5$, $(x_0^7, y_0^7, z_0^4) = (1.939, 0.7655, 12.66)$, (b) $c = -24.5$, $(x_0^8, y_0^8, z_0^4) = (-1.939, -0.7655, 12.66)$, phase portraits of system (3.2), illustrating the existence of hidden two-scroll Lorenz-like attractors coexisting with two stable equilibria in system (3.1) using system (3.2).

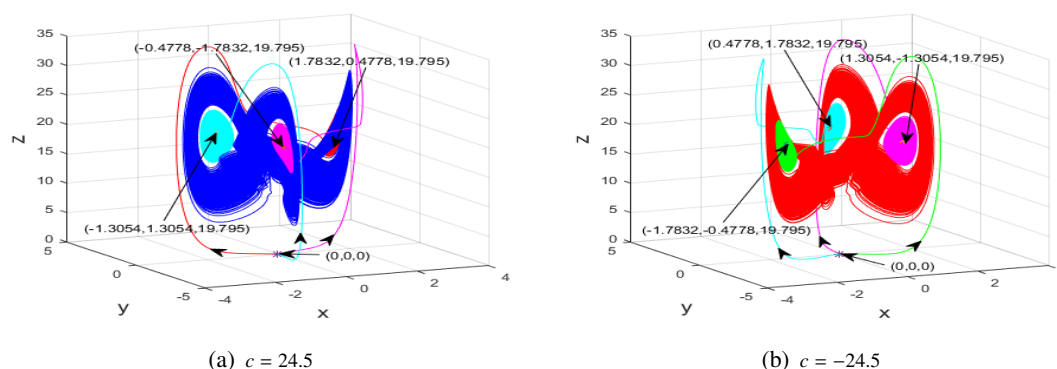


Figure 6. For $(a, b) = (4, 1)$, $(x_0^{5,6}, y_0^{5,6}, z_0^3) = (\pm 1.314, \pm 1.618, 1.618) \times 10^{-4}$, (a) $c = 24.5$, $(x_0^6, y_0^5, z_0^3) = (-1.314, 1.618, 1.618) \times 10^{-4}$, $(x_0^7, y_0^7, z_0^4) = (1.939, 0.7655, 12.66)$, (b) $c = -24.5$, $(x_0^5, y_0^6, z_0^3) = (1.314, -1.618, 1.618) \times 10^{-4}$, $(x_0^8, y_0^8, z_0^4) = (-1.939, -0.7655, 12.66)$, phase portraits of system (3.3), illustrating the existence of hidden three-scroll Lorenz-like attractors coexisting with three stable equilibria in system (3.1) using system (3.3).

Then, combining the dynamics of E_z and numerical simulation, Section 3 discusses asymmetric pseudo singularly degenerate heteroclinic cycles and gives the forming mechanism of hidden single-scroll Lorenz-like attractors illustrated in Figure 3.

At last, the existence of a single heteroclinic orbit to E_0 and E' of system (3.1) is presented in the following proposition, and is proved in Section 4 by aid of two suitable Lyapunov functions, concepts of both an α -limit set and ω -limit set [6, 9, 22–27], as depicted in Figures 7 and 8.

Proposition 3.3. *If $b \geq 2a > 0$ and $c \neq 0$, then system (3.1) has neither closed orbits nor homoclinic orbits, but a single heteroclinic orbit to E_0 and E' .*

Remark 2. *Although system (3.1) exhibits similar dynamics as the six-fifths-degree sub-quadratic Lorenz-like system [9], it creates hidden single-scroll Lorenz-like attractors rather than two-scroll ones due to the six-sevenths-degree term $c\sqrt[7]{x^6}$, extending the generalization of the second part of Hilbert's 16th problem in some degree [7, 8].*

4. Pseudo singularly degenerate heteroclinic cycles with nearby bifurcated hidden single-scroll Lorenz-like attractors

As is known to all, the broken version of pseudo or true singularly degenerate heteroclinic cycles is one forming mechanism of various strange attractors for the Lorenz system family [6, 9, 20–26, 30]. In this endeavor, one tries to study singularly degenerate heteroclinic cycles of system (3.1), aiming at exploring the mechanisms of formation of the aforementioned hidden single-scroll Lorenz-like attractors to some degree.

For this purpose, the following linear transformation

$$T : (x, y, z, t) \rightarrow (20x, 20y, 20z, \frac{1}{20}t)$$

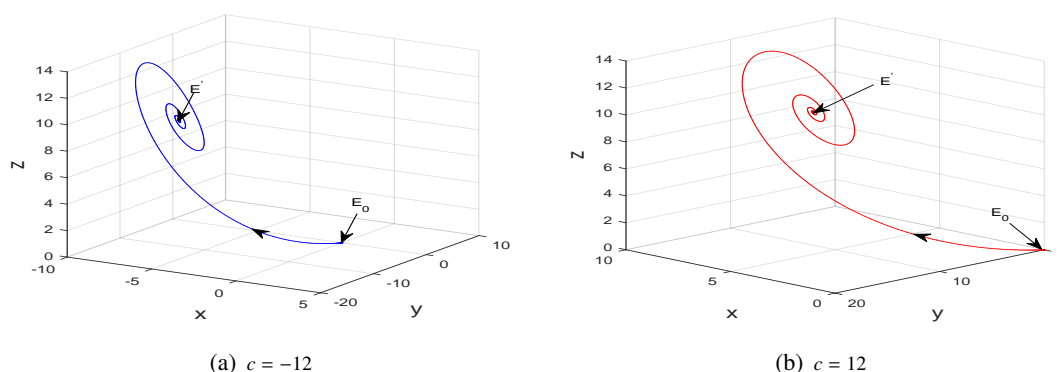


Figure 7. When $(a, b) = (3, 6)$, (a) $c = -12$, $(x_0^2, y_0^2, z_0^1) = (-1.314, -1.618, 1.618) \times 10^{-7}$, (b) $c = 12$, $(x_0^1, y_0^1, z_0^1) = (1.314, 1.618, 1.618) \times 10^{-7}$, a single heteroclinic orbit to E_0 and E' of system (3.1) for $c \neq 0$ and $b = 2a > 0$.

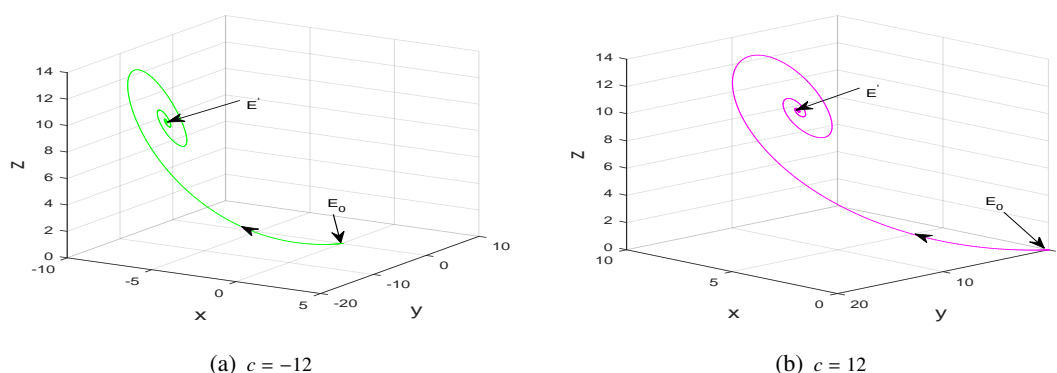


Figure 8. When $(a, b) = (3, 7)$, (a) $c = -12$, $(x_0^2, y_0^2, z_0^1) = (-1.314, -1.618, 1.618) \times 10^{-7}$, (b) $c = 12$, $(x_0^1, y_0^1, z_0^1) = (1.314, 1.618, 1.618) \times 10^{-7}$, a single heteroclinic orbit to E_0 and E' of system (3.1) for $c \neq 0$ and $b > 2a > 0$.

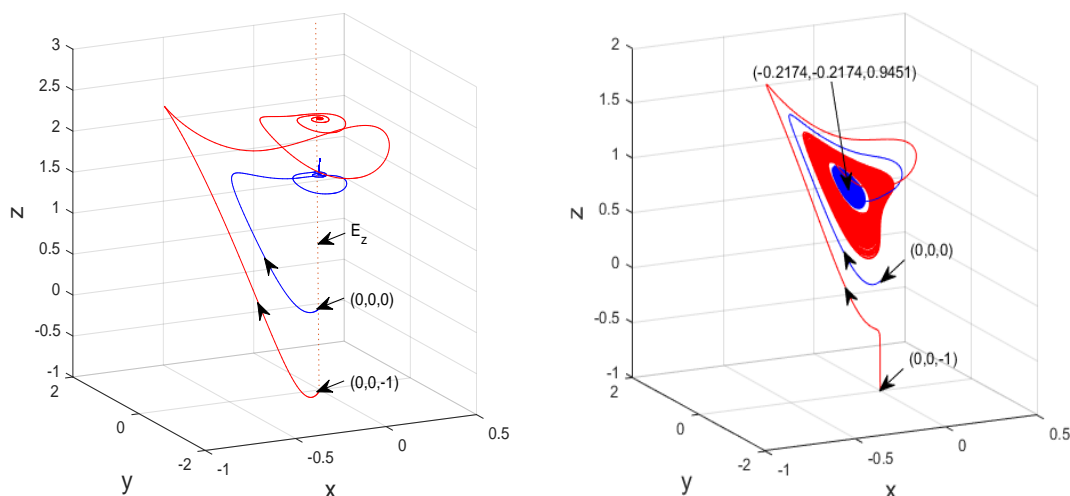
converts system (3.1) into the resulting equivalent system

$$\begin{cases} \dot{x} = \frac{a}{20}(y - x), \\ \dot{y} = \frac{c}{20\sqrt[7]{20}}\sqrt[7]{x^6} - xz, \\ \dot{z} = -\frac{b}{20}z + xy. \end{cases} \quad (4.1)$$

Therefore, the solutions of system (3.1) with $(a, b) = (4, 1)$ and $0 < |c| < 35.5244$ correspond to the ones of system (4.1) with $(\frac{a}{20}, \frac{b}{20}) = (0.2, 0.05)$ and $0 < \frac{|c|}{20\sqrt[7]{20}} < 1.1578$. Combining the dynamics of E_z , E' , and a detailed numerical study, one obtains the following result:

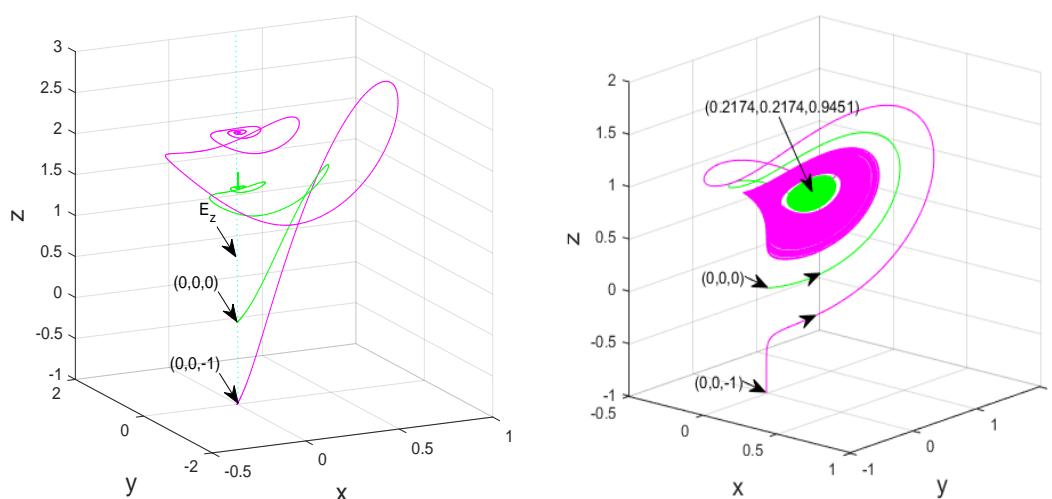
Numerical Result 3.1

When some $|c| \in [0.76, 0.81]$, there may exist potential hidden single-scroll Lorenz-like attractors in system (3.1), as shown in Figures 9–12, which may be created through the collapses of pseudo singularly degenerate heteroclinic cycles as the ones in [22].



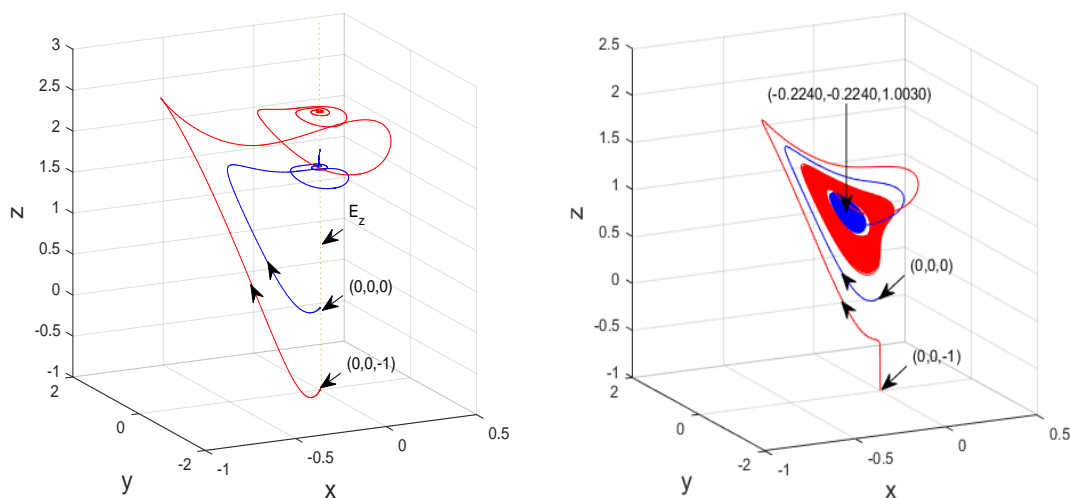
(a) Pseudo singularly degenerate heteroclinic cycles for $(a, c, b) = (0.2, -0.76, 0)$ (b) Stable E' and hidden single-scroll Lorenz-like attractors for $(a, c, b) = (0.2, -0.76, 0.05)$

Figure 9. Phase portraits of system (3.1) with $a = 0.2$, (a) $(c, b) = (-0.76, 0)$, (b) $(c, b) = (-0.76, 0.05)$, $(x_0^2, y_0^2, z_0^1) = (-1.314, -1.618, 1.618) \times 10^{-7}$ (colored in blue), $(x_0^2, y_0^2, z_0^6) = (-1.314 \times 10^{-7}, -1.618 \times 10^{-7}, -1)$ (colored in red), showing pseudo singularly degenerate heteroclinic cycles with the nearby bifurcated hidden single-scroll Lorenz-like attractor.



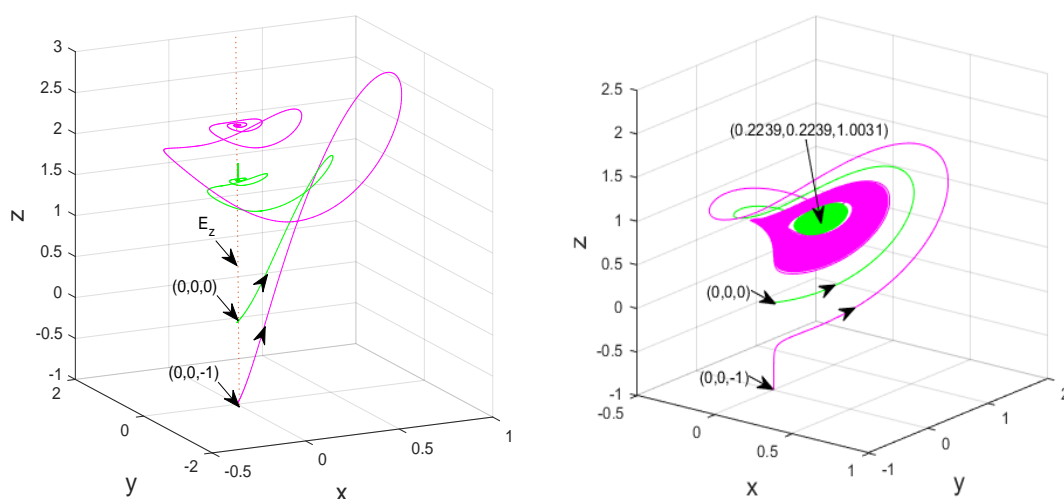
(a) Pseudo singularly degenerate heteroclinic cycles for $(a, c, b) = (0.2, 0.76, 0)$ (b) Stable E' and hidden single-scroll Lorenz-like attractors for $(a, c, b) = (0.2, 0.76, 0.05)$

Figure 10. Phase portraits of system (3.1) with $a = 0.2$, (a) $(c, b) = (0.76, 0)$, (b) $(c, b) = (0.76, 0.05)$, $(x_0^1, y_0^1, z_0^1) = (1.314, 1.618, 1.618) \times 10^{-7}$ (colored in green), $(x_0^1, y_0^1, z_0^6) = (1.314 \times 10^{-7}, 1.618 \times 10^{-7}, -1)$ (colored in magenta), depicting pseudo singularly degenerate heteroclinic cycles with the nearby bifurcated hidden single-scroll Lorenz-like attractor.



(a) Pseudo singularly degenerate heteroclinic cycles for $(a, c, b) = (0.2, -0.81, 0)$ (b) Stable E' and hidden single-scroll Lorenz-like attractors for $(a, c, b) = (0.2, -0.81, 0.05)$

Figure 11. Phase portraits of system (3.1) with $a = 0.2$, (a) $(c, b) = (-0.81, 0)$, (b) $(c, b) = (-0.81, 0.05)$, $(x_0^2, y_0^2, z_0^1) = (-1.314, -1.618, 1.618) \times 10^{-7}$ (colored in blue), $(x_0^2, y_0^2, z_0^6) = (-1.314 \times 10^{-7}, -1.618 \times 10^{-7}, -1)$ (colored in red), showing pseudo singularly degenerate heteroclinic cycles with the nearby bifurcated hidden single-scroll Lorenz-like attractor.



(a) Pseudo singularly degenerate heteroclinic cycles for $(a, c, b) = (0.2, 0.81, 0)$ (b) Stable E' and hidden single-scroll Lorenz-like attractors for $(a, c, b) = (0.2, 0.81, 0.05)$

Figure 12. Phase portraits of system (3.1) with $a = 0.2$, (a) $(c, b) = (0.81, 0)$, (b) $(c, b) = (0.81, 0.05)$, $(x_0^1, y_0^1, z_0^1) = (1.314, 1.618, 1.618) \times 10^{-7}$ (colored in green), $(x_0^1, y_0^1, z_0^6) = (1.314 \times 10^{-7}, 1.618 \times 10^{-7}, -1)$ (colored in magenta), illustrating pseudo singularly degenerate heteroclinic cycles with the nearby bifurcated hidden single-scroll Lorenz-like attractor.

5. Heteroclinic orbit and the proof of Proposition 3.3

In this section, aiming to prove the existence of a unique heteroclinic orbit to E_0 and E' in system (3.1), one first denotes by $\varphi_t(q_0) = (x(t; x_0), y(t; y_0), z(t; z_0))$ a solution of system (3.1) with initial value $q_0 = (x_0, y_0, z_0)$, and by W_-^u (resp. W_+^u) the negative (resp. positive) branch of $W^u(E_0)$ corresponding to $x < 0$ (resp. $x > 0$) when $t \rightarrow -\infty$.

Second, for $c \neq 0$ and $b - 2a \geq 0$, one constructs the following two different Lyapunov functions with their derivatives along $\varphi_t(q_0)$:

(1) Case $b > 2a > 0$

$$\begin{aligned} V_1(\varphi_t(q_0)) &= \frac{1}{2}[b(b-2a)(y-x)^2 + (-bz+x^2)^2 + \frac{b(b-2a)}{2ab}(-\sqrt[15]{(bc)^{14}} + x^2)^2 \\ &+ \frac{7bc(b-2a)}{13a\sqrt[15]{bc}}(-\sqrt[15]{bc}\sqrt[7]{x^6} + x)^2 + \frac{4bc(b-2a)}{13a\sqrt[15]{bc}}(-\sqrt[15]{(bc)^2}\sqrt[7]{x^5} + x)^2 \\ &+ \frac{2bc(b-2a)}{13a\sqrt[15]{bc}}(-\sqrt[15]{(bc)^4}\sqrt[7]{x^3} + x)^2 + \frac{bc(b-2a)\sqrt[15]{bc}}{13a}(-\sqrt[15]{(bc)^6} + \sqrt[7]{x^6})^2] \end{aligned}$$

and

$$\left. \frac{dV_1(\varphi_t(q_0))}{dt} \right|_{(3.1)} = -ab(b-2a)(y-x)^2 - b(-bz+x^2)^2. \quad (5.1)$$

(2) Case $b = 2a > 0$

$$\begin{aligned} V_2(\varphi_t(q_0)) &= \frac{1}{2}[(y-x)^2 + \frac{7c}{13a\sqrt[15]{2ac}}(-\sqrt[15]{2ac}\sqrt[7]{x^6} + x)^2 + \frac{4c}{13a\sqrt[15]{2ac}}(-\sqrt[15]{(2ac)^2}\sqrt[7]{x^5} + x)^2 \\ &+ \frac{2c}{13a\sqrt[15]{2ac}}(-\sqrt[15]{(2ac)^4}\sqrt[7]{x^3} + x)^2 + \frac{c\sqrt[15]{2ac}}{13a}(-\sqrt[15]{(2ac)^6} + \sqrt[7]{x^6})^2 \\ &+ \frac{1}{4a^2}(-\sqrt[15]{(2ac)^{14}} + x^2)^2] \end{aligned}$$

and

$$\left. \frac{dV_2(\varphi_t(q_0))}{dt} \right|_{(3.1)} = -a(y-x)^2. \quad (5.2)$$

Performing similar procedures as in [6, 9, 22–27], we only consider the case of $c < 0$ and $b > 2a > 0$ herein. The other cases are similar and, therefore, are omitted. The key point of this approach lies in proving that the unstable manifolds of E_0 tend to globally stable E' by aid of $V_{1,2}$, which creates a single orbit heteroclinic to E_0 and E' . Aiming at proving Proposition 3.3, one has to introduce the following two assertions.

Proposition 5.1. *If $c < 0$ and $b > 2a > 0$, the following two assertions hold.*

- (a) *If there are t_1 and t_2 such that $t_1 < t_2$ and V_1 satisfies $V_1(\varphi_{t_1}(q_0)) = V_1(\varphi_{t_2}(q_0))$, then $q_0 = E_0$ or $q_0 = E'$.*
- (b) *If $\lim_{t \rightarrow -\infty} \varphi_t(q_0) = E_0$ and $x(t; x_0) < 0$ for some t , then $V_1(E_0) > V_1(\varphi_t(q_0))$ and $x(t; x_0) < 0, \forall t \in \mathbb{R}$, i.e., $q_0 \in W_-^u$.*

Proof. (a) Combining the hypothesis and Eq (5.1), the fact $\left. \frac{dV_1(\varphi_t(q_0))}{dt} \right|_{(3.1)} = 0, \forall t \in (t_1, t_2)$, leads to

$$\dot{x}(t; x_0) \equiv \dot{y}(t; y_0) \equiv \dot{z}(t; z_0) \equiv 0, \quad (5.3)$$

i.e., $q_0 = E_0$ or $q_0 = E'$. Namely, $\varphi_t(q_0) \in \{x=y\} \cap \{bz=x^2\}$ for $b > 2a > 0$ suggests $\dot{x}(t; x_0) \equiv \dot{z}(t; z_0) \equiv 0$. Moreover, the result $y(t) = x(t) = x_0$ leads to $\dot{y}(t; y_0) = 0, \forall t \in \mathbb{R}$.

(b)First, let us prove $V_1(E_0) > V_1(\varphi_t(q_0))$, $\forall t \in \mathbb{R}$. If not, $\exists t_0 \in \mathbb{R}$, $0 < V_1(E_0) \leq V_1(\varphi_{t_0}(q_0))$ holds. Because of $\lim_{t \rightarrow -\infty} \varphi_t(q_0) = E_0$ and the continuity of V_1 in t , $\exists \{t_n\}$, $\lim_{n \rightarrow \infty} t_n = -\infty$, $n_1 > 0$, and one gets $|V_1(\varphi_{t_n}(q_0)) - V_1(E_0)| < \varepsilon$, $\forall \varepsilon > 0$ and $n > n_1$. Due to $\lim_{n \rightarrow \infty} t_n = -\infty$ and $t_0 \in \mathbb{R}$, $\exists n_2 > 0$, one obtains $t_n < t_0$, $\forall n > \max\{n_1, n_2\}$. Moreover, set $n^0 = \max\{n_1, n_2\}$ and $\varepsilon = \frac{1}{2}[V_1(\varphi_{t_0}(q_0)) - V_1(E_0)] \geq 0$. Therefore, $V_1(\varphi_{t_n}(q_0)) - V_1(\varphi_{t_0}(q_0)) = V_1(\varphi_{t_n}(q_0)) - V_1(E_0) + V_1(E_0) - V_1(\varphi_{t_0}(q_0)) < \varepsilon + V_1(E_0) - V_1(\varphi_{t_0}(q_0)) = -\varepsilon \leq 0$ is true. Instead, since $\left. \frac{dV_1(\varphi_t(q_0))}{dt} \right|_{(3.1)} \leq 0$, $V_1(\varphi_{t_n}(q_0)) \geq V_1(\varphi_{t_0}(q_0))$ holds, $\forall t_n < t_0$, $n > n^0$. Accordingly, the fact that $V_1(\varphi_{t_n}(q_0)) = V_1(\varphi_{t_0}(q_0))$ and the first hypothesis (a) result in $q_0 = E_0$ or $q_0 = E'$. Because $\lim_{t \rightarrow -\infty} \varphi_t(q_0) \rightarrow E_0$, $q_0 \equiv E_0$ and $x(t, x_0) \equiv 0$ holds, $\forall t \in \mathbb{R}$. On the basis of the second hypothesis (b), one has $x(t, x_0) < 0$, $\exists t \in \mathbb{R}$. A contradiction occurs. Therefore, $V_1(E_0) > V_1(\varphi_t(q_0))$ is true, $\forall t \in \mathbb{R}$.

Next, we prove $x(t, x_0) < 0$, $\forall t \in \mathbb{R}$. In fact, if $\exists t' \in \mathbb{R}$ and $x(t', x_0) \geq 0$, one obtains $x(\tau, x_0) = 0$, $\exists \tau \in \mathbb{R}$, based on the second hypothesis (b), i.e., $x(t'', x_0) < 0$, $\exists t'' \in \mathbb{R}$. Since $V_1(E_0) > V_1(\varphi_t(q_0))$, $\forall t \in \mathbb{R}$, we derive $\varphi_\tau(q_0) \in \{(x, y, z) : V_1(E_0) > V_1(x, y, z)\} \cap \{x = 0\} = \{(x, y, z) : \frac{1}{2}[b(b-2a)y^2 + (bz)^2 + \frac{bc(b-2a)}{13a}\sqrt[15]{(bc)^{13}} + \frac{b(b-2a)}{2ab}\sqrt[15]{(bc)^{28}}] < \frac{15bc(b-2a)}{52a}\sqrt[15]{(bc)^{13}}\} = \emptyset$, which leads to $x(t, x_0) < 0$, $\forall t \in \mathbb{R}$. This completes the proof. \square

Finally, the proof of Proposition 3.3 follows from Proposition 5.1.

Proof. Herein, one only considers the cases of $c < 0$ and $b > 2a > 0$. The proofs of other cases, i.e., (i) $c > 0$ and $b > 2a > 0$, (ii) $c \neq 0$ and $b = 2a > 0$, are similar and, therefore, are omitted.

Since $\left. \frac{dV_1(\varphi_t(q_0))}{dt} \right|_{(3.1)} \leq 0$, we obtain

$$0 \leq V_1(\varphi_t(q_0)) \leq V_1(q_0), \quad (5.4)$$

and that the limit $\lim_{t \rightarrow +\infty} V_1(\varphi_t(q_0)) = V_1^*(q_0)$ exists, which suggests the boundedness of $\varphi_t(q_0) = (x(t, x_0), y(t, y_0), z(t, z_0))$, $\forall t \geq 0$. Set $\Omega(q_0)$ to be the ω -limit set of $\varphi_t(q_0)$, i.e., $\varphi_t(q) \in \Omega(q_0)$, $\forall q \in \Omega(q_0)$. As a result, $\forall \varphi_t(q)$, $t \geq 0$, $\exists t_n \rightarrow \infty$, $\lim_{n \rightarrow +\infty} \varphi_{t_n}(q_0) = \varphi_t(q)$ holds, i.e.,

$$V_1(\varphi_t(q)) = \lim_{n \rightarrow +\infty} V_1(\varphi_{t_n}(q_0)) = V_1^*(q_0) = \text{const},$$

$\forall t \geq 0$. In light of Proposition 5.1, $q = E_0$ or E' , i.e., closed orbits are nonexistent.

Next, set $\gamma(t, q_0)$ to be a homoclinic orbit to E_0 or E' , i.e., $\lim_{t \rightarrow \pm\infty} \gamma(t, q_0) = m$, where $q_0 \notin \{E_0, E'\}$ and $m \in \{E_0, E'\}$. Due to $\left. \frac{dV_1(\varphi_t(q_0))}{dt} \right|_{(3.1)} \leq 0$, we obtain

$$0 \leq V_1(m) = V_1(\gamma(-\infty, q_0)) \leq V_1(\gamma(t, q_0)) \leq V_1(\gamma(\infty, q_0)) = V_1(m),$$

i.e., $V_1(\gamma(t, q_0)) = V_1(m)$, $\forall t \in \mathbb{R}$. On the basis of Proposition 5.1, we get $q_0 \in \{E_0, E'\}$. A contraction occurs. Therefore, homoclinic orbits are nonexistent in system (3.1).

Since $V_1(E_0) > V_1(E')$, each one-dimensional branch of W_-^u has a ω -limit, which is nothing but E' and thus forms a unique heteroclinic orbit to E_0 and E' . Figure 8(a) also validates the correctness of that theoretical result. \square

6. Conclusions

How to coin novel strange attractors is an interesting problem, especially the hidden n -scroll Lorenz-like ones coexisting with n stable equilibria. In the sense of generalization of the second part of Hilbert's celebrated 16th problem, we introduced a new Lorenz-like system with the nonlinear term $\sqrt[7]{x^6}$ and cross products xy and xz , which presents the following complex dynamics: (1) hidden single-scroll Lorenz-like attractors coexisting with the unstable E_0 and stable E' ; (2) pseudo singularly degenerate heteroclinic cycles with nearby bifurcated hidden single-scroll Lorenz-like attractors; (3) the existence of a single heteroclinic orbit to E_0 and E' . In contrast to the Lorenz-like systems [6, 9, 24], the degree determines not only the number and mutual position, but also the geometrical structure of Lorenz-like attractors.

Through the fractal process or rotation symmetry of the proposed system, there may exist hidden n -scroll Lorenz-like attractors coexisting with n stable equilibria using the resulting system. Here, we presented two examples of hidden two/three-scroll Lorenz-like attractors coexisting with two/three stable equilibria. In contrast to the spiralling attractor near heteroclinic networks that contains two hyperbolic equilibria, heteroclinic trajectories connecting them transversely, and a non-trivial hyperbolic, invariant, and transitive set [31], the newly reported single-scroll hidden one only coexists with a single orbit heteroclinic to the unstable E_0 and locally stable E' , and n -scroll hidden ones only coexist with n locally stable nontrivial equilibrium points ($n \geq 2$), which lead to the nonexistence of heteroclinic networks.

Notably, the aforementioned hidden Lorenz-like attractors are only numerical results that can not be simulated for a long time, which leads to a dilemma that one could not determine whether or not they are true or transient chaos.

Conjecture 6.1. *Does the dynamics of system (3.1) match that of the geometric hidden single-scroll Lorenz-like attractors shown in Figure 3? Furthermore, when the created 2/3-scroll Lorenz-like attractors coexist with 2/3 stable nontrivial equilibria depicted in Figures 5 and 6 under fractal process or rotation symmetry (i.e., the mapping Ψ_n), are they hidden sustained attractors or hidden transient chaotic sets?*

Therefore, one needs to study the topological horseshoes of them and thus rigorously prove the existence of chaos. In addition, the relationship between hidden attractors and the degree, singular orbits, invariant algebraic surfaces, practical applications, and so on, deserve consideration in future work.

Use of AI tools declaration

The authors declare they have not used Artificial Intelligence (AI) tools in the creation of this article.

Acknowledgments

This work is supported in part by the Zhejiang Public Welfare Technology Application Research Project of China under Grant LGN21F020003, in part by the National Natural Science Foundation of China under Grant 12001489, in part by the Natural Science Foundation of Taizhou University under Grant T20210906033. Meanwhile, the authors would like to express their sincere thanks to the anonymous editors and reviewers for their conscientious reading and numerous constructive comments which improved the manuscript substantially.

Conflict of interest

The authors declare there are no conflicts of interest.

Data availability

All data generated or analyzed during this study are included in this published article.

References

1. R. Miranda, E. Stone, The proto-Lorenz system, *Phys. Lett. A*, **178** (1993), 105–113. [https://doi.org/10.1016/0375-9601\(93\)90735-I](https://doi.org/10.1016/0375-9601(93)90735-I)
2. C. Letellier, P. Werny, J. M. Malasoma, R. Gilmore, Multichannel intermittencies induced by symmetries, *Phys. Rev. E*, **66** (2002), 036220. <https://doi.org/10.1103/PhysRevE.66.036220>
3. Y. Guo, G. Qi, Y. Hamam, A multi-wing spherical chaotic system using fractal process, *Nonlinear Dyn.*, **85** (2016), 2765–2775. <https://doi.org/10.1007/s11071-016-2861-7>
4. Y. Yang, L. Huang, J. Xiang, H. Bao, H. Li, Design of multi-wing 3D chaotic systems with only stable equilibria or no equilibrium point using rotation symmetry, *Int. J. Electron. Commun.*, **135** (2021), 153710. <https://doi.org/10.1016/j.aeue.2021.153710>
5. M. Marwan, A. Xiong, M. Han, R. Khan, Chaotic behavior of Lorenz-based chemical system under the influence of fractals, *MATCH Commun. Math. Comput. Chem.*, **91** (2024), 307–336. <https://doi.org/10.46793/match.91-2.307M>
6. J. Pan, H. Wang, G. Ke, F. Hu, Creation of single-wing Lorenz-like attractors via a ten-ninths-degree term, *Open Phys.*, **23** (2025), 20250165. <https://doi.org/10.1515/phys-2025-0165>
7. N. V. Kuznetsov, T. N. Mokaev, O. A. Kuznetsova, E. V. Kudryashova, The Lorenz system: Hidden boundary of practical stability and the Lyapunov dimension, *Nonlinear Dyn.*, **102** (2020), 713–732. <https://doi.org/10.1007/s11071-020-05856-4>
8. X. Zhang, G. Chen, Constructing an autonomous system with infinitely many chaotic attractors, *Chaos Interdiscip. J. Nonlinear Sci.*, **27** (2017), 071101. <https://doi.org/10.1063/1.4986356>
9. H. Wang, J. Pan, G. Ke, Revealing more hidden attractors from a new sub-quadratic Lorenz-like system of degree $\frac{6}{5}$, *Int. J. Bifurcation Chaos*, **34** (2024), 2450071. <https://doi.org/10.1142/s0218127424500718>
10. S. Jafari, J. C. Sprott, F. Nazarimehr, Recent new examples of hidden attractors, *Eur. Phys. J. Spec. Top.*, **224** (2015), 1469–1476. <https://doi.org/10.1140/epjst/e2015-02472-1>
11. D. Dudkowski, S. Jafari, T. Kapitaniak, N. V. Kuznetsov, G. A. Leonov, A. Prasad, Hidden attractors in dynamical systems, *Phys. Rep.*, **637** (2016), 1–50. <https://doi.org/10.1016/j.physrep.2016.05.002>
12. S. N. Chowdhury, D. Ghosh, Hidden attractors: A new chaotic system without equilibria, *Eur. Phys. J. Spec. Top.*, **229** (2020), 1299–1308. <https://doi.org/10.1140/epjst/e2020-900166-7>
13. S. N. Chowdhury, S. Kundu, M. Perc, D. Ghosh, Complex evolutionary dynamics due to punishment and free space in ecological multigames, *Proc. R. Soc. A*, **477** (2021), 20210397. <https://doi.org/10.1098/rspa.2021.0397>

14. C. Wang, Y. Li, Q. Deng, Discrete-time fractional-order local active memristor-based Hopfield neural network and its FPGA implementation, *Chaos Solitons Fractals*, **193** (2025), 116053. <https://doi.org/10.1016/j.chaos.2025.116053>
15. Q. Deng, C. Wang, G. Yang, Chaotic dynamics of memristor-coupled tabu learning neuronal network, *Int. J. Bifurcation Chaos*, **35** (2025), 25500531. <https://doi.org/10.1142/S0218127425500531>
16. Q. Deng, C. Wang, Y. Sun, G. Yang, Memristive multi-wing chaotic hopfield neural network for LiDAR data security, *Nonlinear Dyn.*, **113** (2025), 17161–17176. <https://doi.org/10.1007/s11071-025-10982-y>
17. S. L. Brunton, J. L. Proctor, J. N. Kutz, Discovering governing equations from data by sparse identification of nonlinear dynamical systems, *PNAS*, **113** (2016), 3932–3937. <https://doi.org/10.1073/pnas.1517384113>
18. P. Dubois, T. Gomez, L. Planckaert, L. Perret, Data-driven predictions of the Lorenz system, *Phys. D*, **408** (2020), 132495. <https://doi.org/10.1016/j.physd.2020.132495>
19. J. C. Sprott, A proposed standard for the publication of new chaotic systems, *Int. J. Bifurcation Chaos*, **21** (2011), 2391–2394. <https://doi.org/10.1142/S021812741103009X>
20. Y. Chen, Q. Yang, A new Lorenz-type hyperchaotic system with a curve of equilibrium, *Math. Comput. Simul.*, **112** (2015), 40–55. <https://doi.org/10.1016/j.matcom.2014.11.006>
21. H. Kokubu, R. Roussarie, Existence of a singularly degenerate heteroclinic cycle in the Lorenz system and its dynamical consequences: Part I, *J. Dyn. Differ. Equations*, **16** (2004), 513–557. <https://doi.org/10.1007/s10884-004-4290-4>
22. H. Wang, G. Ke, F. Hu, J. Pan, G. Dong, G. Chen, Pseudo and true singularly degenerate heteroclinic cycles of a new 3D cubic Lorenz-like system, *Results Phys.*, **56** (2024), 107243. <https://doi.org/10.1016/j.rinp.2023.107243>
23. H. Wang, G. Ke, J. Pan, Q. Su, Conjoined Lorenz-like attractors coined, *Miskolc Math. Notes*, **26** (2025), 527–546. <https://doi.org/10.18514/MMN.2025.4489>
24. H. Wang, J. Pan, G. Ke, F. Hu, A pair of centro-symmetric heteroclinic orbits coined, *Adv. Contin. Discrete Models*, **2024** (2024), 1–11. <https://doi.org/10.1186/s13662-024-03809-4>
25. H. Wang, J. Pan, F. Hu, G. Ke, Asymmetric singularly degenerate heteroclinic cycles, *Int. J. Bifurcation Chaos*, **35** (2025), 2550072. <https://doi.org/10.1142/S0218127425500725>
26. J. Pan, H. Wang, G. Ke, F. Hu, A novel Lorenz-like attractor and stability and equilibrium analysis, *Axioms*, **14** (2025), 264. <https://doi.org/10.3390/axioms14040264>
27. J. Pan, H. Wang, F. Hu, Revealing asymmetric homoclinic and heteroclinic orbits, *Electron. Res. Arch.*, **33** (2025), 1337–1350. <https://doi.org/10.3934/era.2025061>
28. Y. A. Kuznetsov, *Elements of Applied Bifurcation Theory*, Springer-Verlag, New York, 2004. <https://doi.org/10.1007/978-1-4757-3978-7>
29. J. Sotomayor, L. F. Mello, D. C. Braga, Lyapunov coefficients for degenerate Hopf bifurcations, preprint, arXiv:0709.3949. <https://doi.org/10.48550/arXiv.0709.3949>

-
30. H. Wang, G. Ke, G. Dong, Q. Su, J. Pan, Singularly degenerate heteroclinic cycles with nearby apple-shape attractors, *Int. J. Bifurcation Chaos*, **33** (2023), 2350011. <https://doi.org/10.1142/S0218127423500116>
 31. A. A. P. Rodrigues, I. S. Labouriau, Spiralling dynamics near heteroclinic networks, *Phys. D*, **268** (2014), 34–49. <https://doi.org/10.1016/j.physd.2013.10.012>



AIMS Press

©2025 the Author(s), licensee AIMS Press. This is an open access article distributed under the terms of the Creative Commons Attribution License (<https://creativecommons.org/licenses/by/4.0>)